Phosphorus–Bismuth *peri*-Substituted Acenaphthenes: A Synthetic, Structural and Computational Study

Phillip S. Nejman,[a] Thomasine E. Curzon,[a] Michael Bühl,[a] David McKay,[a] J. Derek Woollins,[b] Sharon E. Ashbrook,[a] David B. Cordes,[a] Alexandra M. Z. Slawin,[a] Petr Kilian*[a]

a EaStChem School of Chemistry, University of St Andrews, St Andrews, Fife KY16 ST, UK

b Dept. of Chemistry, Khalifa University, PO Box 127788, Abu Dhabi, UAE

Abstract

A series of acenaphthene species with a diisopropylphosphino group and a variety of bismuth functionalities in the *peri*-positions were synthesised and fully characterised, including single crystal X-ray diffraction. The majority of the reported species feature a relatively rare interpnictogen P−Bi bond. The series includes the phosphine−bismuthine, Acenap(P*i*Pr$_2$)(BiPh$_2$) **2** (Acenap = acenaphthene-5,6-diyl), which was subjected to a fluorodearylation reaction to produce Acenap(P*i*Pr$_2$)(BiPhX) **5**–**8** and **10** (X = BF_4^-, Cl, Br, I, SPh), displaying varying degrees of ionicity. The geminally bis(acenaphthyl) substituted [Acenap(P*i*Pr$_2$)$_2$]BiPh **3** shows a large through-space coupling of 17.8 Hz, formally $^{8ts}J_{PP}$. Coupling deformation density (CDD) calculations confirm the double through-space coupling pathway, in which the P and Bi lone pairs mediate communication between the two ^{31}P nuclei. Several synthetic routes towards the phosphine−diiodobismuthine Acenap(P*i*Pr$_2$)(BiI$_2$) **9** have been investigated, however the purity of this, surprisingly thermally stable potential synthon, remains poor.

Introduction

Whilst phosphines, as well as their heavier pnictine congeners, arsines, stibines and bismuthines, are generally used as (strong and soft) Lewis bases, they can also act as (generally modest and soft) Lewis acids. Their Lewis acidity is driven by the substituent effects, for example halopnictines are Lewis acidic, whilst trialkyl- or triarylpnictines generally do not display Lewis acidity and are more basic in character.[1-6] The dative complexes R$_3$E→E'R'$_3$, where one pnictine (R$_3$E) acts as a Lewis base and another pnictine (E'R'$_3$) as a Lewis acid, are an interesting compound class, demonstrating the mentioned ambiphilic character of pnictines. Many of the pnictine−pnictine complexes are redox unstable, for example, the halophosphines tend to oxidise the alkylphosphines at well below room

temperature.[7-8] Nevertheless, a number of $R_3E\rightarrow E'R'_3$ dative species have been either isolated or observed spectroscopically and they have been treated in several reviews.[9-14] Structural and spectroscopic data indicate these complexes adopt a variety of structural forms, including one,[15] two[16] and even three[17] pnictine ligands being coordinated to the Lewis acidic pnictine centre. This results in the general molecular formulae $R_3E\rightarrow E'R'_3$, $(R_3E\rightarrow)_2E'R'_3$ and $(R_3E\rightarrow)_3E'R'_3$. The pnictine−pnictine dative complexes also display differing aggregation, which in the solid state manifests by a formation of monomers,[17] dimers,[15] oligomers,[18] and polymers.[19] The aggregation generally takes place through one or more bridging halogen atoms. Additionally, pnictine−pnictine dative complexes show varying degrees of ionic character, both in solution and the solid state. This stems from dissociation at the Lewis acidic site leading to an equilibrium between the molecular $R_3E\rightarrow E'X_3$ and ionic $(R_3E\rightarrow E'X_2)^+X^-$ forms, with X^- being a weakly bound halide, or a less coordinating group, such as triflate or hexafluorophosphate.[20] As a result, permutations of the structural variables mentioned above allow these dative compounds to adopt a large variety of structures. Considering that some of the pnictogen−pnictogen dative bonds are relatively weak and that the energy separating the aggregated forms and the ionic/molecular forms is only small (and comparable to crystal packing effects), it is rather difficult to predict which of the many possible structures the species will adopt in each case.

We have a long-term interest in *peri*-substitution chemistry,[21-22] and more recently have become interested in attaching heavy pnictogens, in particular antimony and bismuth,[23-24] onto the acenaphthene scaffold. To date, only four examples of species with bismuth and a non-hydrogen atom in the *peri*-positions of either naphthalene or acenaphthene have been reported in CCDC,[25] with the other (non-hydrogen) atom in the *peri*-region being phosphorus (three examples)[15, 26-27] and boron.[28] More surprisingly, only 30 species containing P−Bi bond have been reported in CCDC, with approximately half of these containing formally dative P→Bi bonds. Selected examples of the latter, illustrating some of the structural variety in this compound class, are shown in Figure 1. The *peri*-substituted species **A**, in which the Bi atom is coordinated to only one phosphine donor, forms a dimer with two bridging chlorine atoms.[15] The crystal structure by Willey (CSD-RABNAF)[17] consists of co-crystallised molecules of a bioctahedral dimer **B**, in which each Bi atom accepts two phosphine donor atoms and **C,** a bis(phosphine) ligand linked molecule, in which each Bi atom accepts three phosphine donor atoms. A monomeric species is observed in the solid state structure of **D**, in which the weakly coordinating PF_6^- anion is ionically separated.[29]

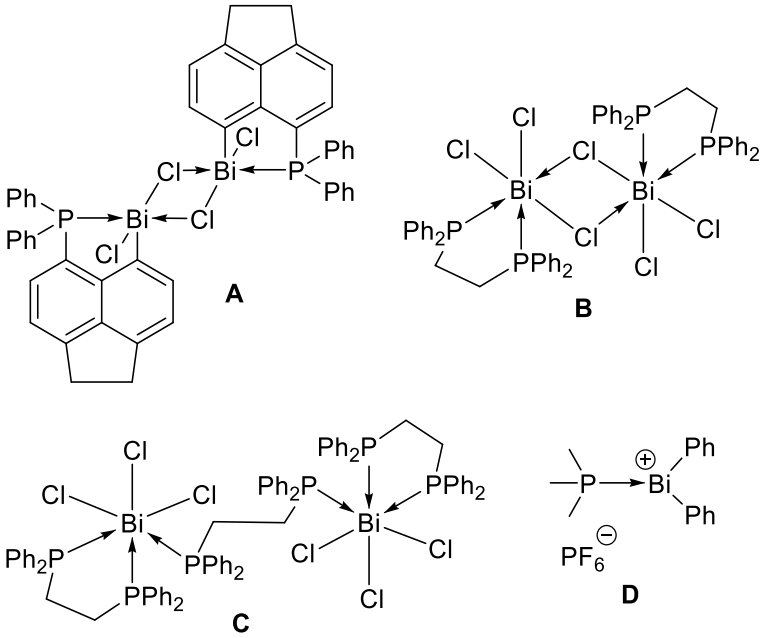

Figure 1 Selected phosphine−bismuthine species, illustrating the variety of the structural motifs of pnictine−pnictine dative species.

It has been shown that the enforced proximity of the donor and acceptor centres in *peri*-substituted species enhances the dative interaction and may lead to unusual reactivity, including stabilisation of normally fleeting motifs.[30] This work will expand the series of *peri*-substituted phosphino−bismuthines via syntheses of species formed by a (formal) halogen displacement in $XBiPh_2$, X_2BiPh and X_3Bi (X = halogen) by an Acenap(P*i*Pr$_2$) group, with a view of gaining access to a wider variety of synthetically valuable species. It will also explore the factors driving the variety of structural motifs observed in this class of compounds.

Results and Discussion

A salt elimination reaction of aryllithiums with electrophilic pnictogen(III) halides is widely used in the formation of lighter C−E bonds, such as C−P or C−As bonds.[31] In our efforts to expand the *peri*-substitution chemistry of bismuth, the reactions of Acenap(P*i*Pr$_2$)Li (**1**) with bismuth(III) halide reagents Ph_2BiCl, $PhBiCl_2$, $BiCl_3$ and BiI_3 were investigated. Observed limitations in this approach included lack of access to the arylhalide precursor $PhBiCl_2$ in good purity, and difficulty to achieve desired selectivity for mono- or disubstitution in the cases of reactions with multifunctional electrophiles ($PhBiCl_2$ and $BiCl_3$).

Phosphino–Bismuthine 2

Ph_2BiCl was prepared by a redistribution reaction of $BiPh_3$ and $BiCl_3$ in a 2:1 stoichiometric ratio.[32-33] The reaction was performed on a multigram scale, affording analytically pure material.

The subsequent reaction of Acenap(P*i*Pr$_2$)Li, **1**, with Ph_2BiCl proceeded cleanly giving phosphine–bismuthine **2** (Scheme 1). Analytically pure material was obtained after recrystallisation from hot acetonitrile. The reaction was performed more than ten times, in these attempts the yields varied from 13 to 60% with the differences in yields appearing for no obvious reason. Using larger scale (starting from multigram quantities of **1**) generally gave higher yields. The $^{31}P\{^1H\}$ NMR spectrum of **2** showed a sharp singlet at δ_P −23.7 ppm, indicating a fairly shielded phosphorus environment. The $^{13}C\{^1H\}$ NMR spectrum of **2** displayed two signals for the CH_3 and one for the CH motifs of the isopropyl groups, in line with the C_S symmetry of **2**. Interestingly, the phenyl *ipso*-carbon signal appears as a doublet due to coupling to the phosphorus atom. The large $^{5ts}J_{CP}$ value of 42.2 Hz likely consists of a dominant contribution from a through-space P···Bi–C coupling pathway (as indicated by the '5ts' superscript).

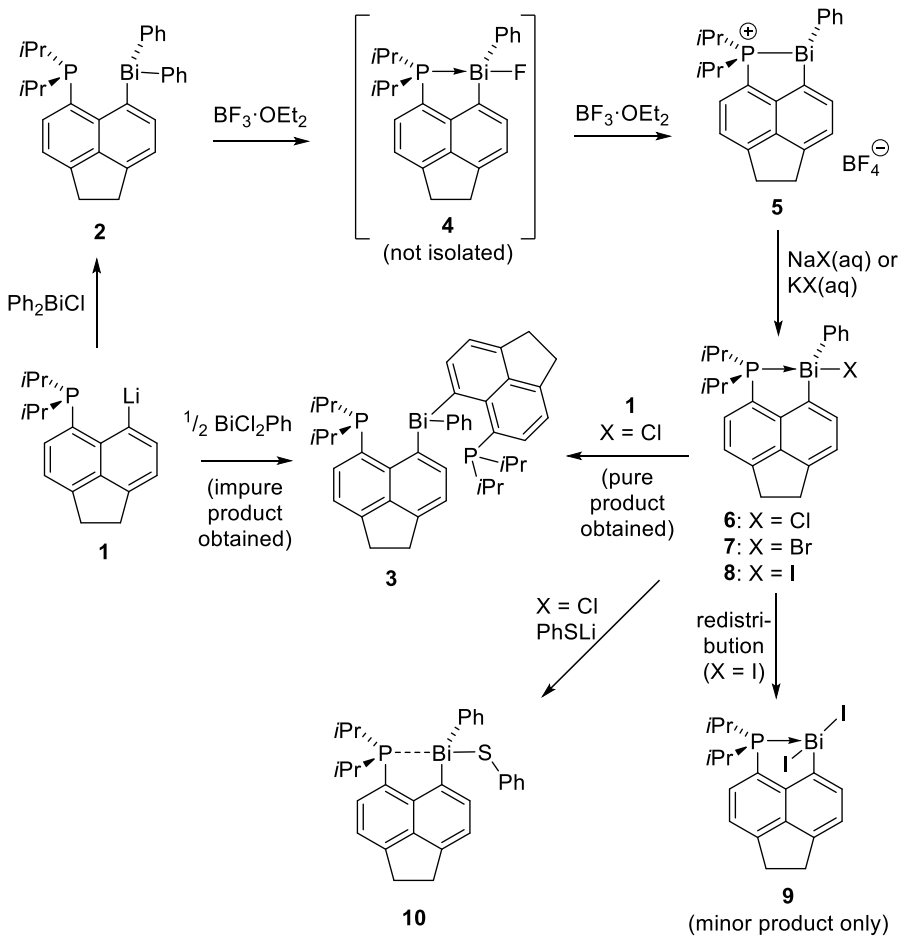

Scheme 1: Syntheses reported in this work. For additional syntheses see also Scheme 2.

The crystal structure of **2** is shown in Figure 3 with selected structural parameters listed in Table 1. Compound **2**, like all structures in this paper, displays angles around Bi atom close to 90 or 180°, indicating the lone pair on the bismuth atom is diffuse with weak stereochemical activity. This is in line with many other Bi^{III} compounds reported in the literature, such as amine adducts of bismuth halides reported by Norman.[34] The P9···Bi1 distance of 3.263(2) Å in **2** accounts to 77% of the sum of the respective van der Waals radii.[35] Despite this, it is significantly longer (by 22%) compared to a "conventional" P−Bi bond seen in bismuthine−phosphonium species **D** (P−Bi distance of 2.667(2) Å).[29] This indicates only weak (if any) attractive P···Bi interaction is present. A quasi-linear arrangement of P9···Bi1−C13 motif (161.5(5)°) indicates the onset of a 3c–4e type interaction with partial transfer of the phosphorus lone pair density into the antibonding Bi–C orbital (n(P)→σ*(Bi−C)).

Tetrafluoroborate salt 5, halides 6–8 and sulfide 10

A fluorodearylation reaction to form a nitrogen donor–bismuth acceptor complex was reported by Suzuki.[36] This synthetic strategy has been extended to our phosphino−bismuthine chemistry. Treatment of **2** with $BF_3{\cdot}OEt_2$ gave bismuthine−phosphonium **5** in an 86% yield. The tetrafluoroborate anion is likely to be formed via abstraction of fluoride (by BF_3) from the transiently formed fluorobismuthine **4** (see Scheme 1).

Subsequently, three halo-bismuthines **6**–**8** were prepared in very good yields (77−86%) via treating a dichloromethane solution of tetrafluoroborate salt **5** with an excess of the respective sodium or potassium halide in the form of an aqueous solution (Scheme 1). The compounds were obtained as either white (**6** and **7**) or yellow (**8**) solids. In all cases the compounds required no further purification. The compounds were found to be stable in a $CDCl_3$ solution for several days before decomposition products started to appear in both the ^{1}H and $^{31}P\{^{1}H\}$ NMR spectra. Several attempts were made to prepare the fluorine derivative by treating **5** with a saturated aqueous potassium fluoride solution. On each occasion, a mixture of products was obtained as judged by the $^{31}P\{^{1}H\}$ NMR spectrum. For this reason, this synthetic target was not pursued further.

The $^{31}P\{^{1}H\}$ NMR spectrum of **5** shows a singlet at δ_P 56.6 ppm, which is rather strongly deshielded compared to the shifts observed for **6**–**8** (δ_P 18.8 (**6**), 15.4 (**7**) and 12.9 ppm (**8**)). This is consistent with the differing (*i.e.* ionic) structure of **5** in the solution as opposed to molecular structures of **6**–**8**. Single crystal X-ray diffraction of **5** (see Figure 3 and Table 1) showed the BF_4^- anion is ionically separated from the complex cation, albeit with relatively short Bi···F closest contact (2.76 Å). This contrasts with the crystal structures of compounds **6**–**8**, which are molecular, with the

halide atoms attached to bismuth atom covalently, be it somewhat loosely. The Bi−X bonds in **6**−**8** are elongated by 0.17 to 0.30 Å, compared to the respective bonds in the bismuth diaryl halides Ar_2BiCl (Ar = 2,4,6-tris(trifluoromethyl)phenyl),[37] Mes_2BiBr (Mes = mesityl, 2,4,6-trimethylphenyl)[38] and the pyridine complex [Ph_2BiI(4-Mepy)] (4-Mepy = 4-methylpyridine).[34] Notably, the Bi−Cl bond distance (2.768(2) Å) in **6** is comparable to the shortest Bi···F contact (2.736(4) Å) in the tetrafluoroborate salt **5**, indicating all of these compounds are close to the ionic-covalent borderline.

The bismuth coordination geometry in **5** is distorted trigonal pyramidal, with all angles close to 90°. If the loose contact to the most proximate fluorine atom is considered as being part of the coordination sphere, a distorted disphenoidal geometry is obtained with P9−Bi1···F1 angle of 163.1(5)°. The same (distorted disphenoidal) geometry around bismuth atom is observed in **6**−**8**; in these cases, the halogen atoms are covalently attached to the bismuth atom as discussed above. No secondary intermolecular Bi···X interactions are observed in any of the halide compounds **6**−**8**, *i.e.* the compounds are monomeric in the solid state. The P−Bi bond length in **5** is significantly shorter (2.674(2) Å) than those in **6**−**8** (2.816(2) Å in **6**, 2.819(3) Å in **7** and 2.798(1) Å in **8**), which again supports interpretation of the bonding as ionic in **5** and covalent in **6**−**8**.

Chlorobismuthine **6** was probed for its reactivity with PhSLi. The reaction proceeded cleanly affording sulfide **10** in a good yield. The crystal structure of **10** is shown in Figure 3 and Table 1. The observed P−Bi bond length (2.9999(5) Å) indicates compound **10** adopts an intermediate structure between the partially ionically separated **6**−**8** series and the fully molecular **2** and **3**. The P9−Bi1−S1 motif is close to linear (171.01(2)°) as seen in the halides **6**−**8**.

To complement these findings, we performed density functional calculations at a level compatible with that in our previous work (B3LYP/SDD/6-31(+)G* level).[23, 39] Optimised P−Bi and Bi−X distances (X = halogen in **4**−**9**, *ipso*-carbon in **2** and **3**, sulfur in **10**) and Wiberg bond indices (WBIs)[40] are collected in Table 1. Consistent with results for related P−Sn[39] and P−Sb species,[23] the P−Bi distances in compounds with a halogen atom *trans* to the phosphorus atom depend considerably on the surrounding medium. These distances, when optimized in the gas phase, are significantly overestimated with respect to the values observed in the solid (by up to 0.161 Å, see entry for **5** in Table 1). They shorten significantly when optimized in a continuum modelling a moderately polar solvent (chloroform in this case). Compounds without halogen atoms in the *trans* position are much less affected by the environment (see for instance values for **2** and **3** in Table 1). This observation is readily explained by a shift in the equilibrium between molecular and ionic resonance structures P: Bi−X ↔ P^+−Bi :X^-, where a polar environment favours the ionic resonance structure on the right. Contributions from this resonance structure are reflected in the charge

distribution and, in particular, the molecular dipole moment, which adopts high values for **4**, **6**–**8** and **10** (exceeding 16 D) and an even larger value for **5** (22 D, last entry in Table 1). The WBIs, which are a measure for the covalent character of a bond, are in line with this interpretation. For many of the compounds substantial values are obtained for P-Bi bonds, whereas WBIs significantly smaller than 1 are obtained for Bi-X bonds (see values in square brackets in Table 1).

Table 1 Selected distances [Å], bond angles and torsion angles [°] observed in the solids and calculated at the B3LYP(-D3)/SDD/6-31(+)G* level. Wiberg bond indices obtained at the same level for the respective set of structures are given in square brackets. Also shown are quantities from population and NBO analyses, natural charges for the atoms indicated and dipole moments in Debye. X = halogen in **4**–**9**, *ipso*-carbon in **2** and **3**, sulfur in **10**.

	2[a]	**3**	**4**	**5**	**5a**[b]	**6**	**7**	**8**	**9**[c]	**10**
Distances										
P–Bi$_{X\text{-}ray}$	*3.2623(2)*	*3.227(2)*[d] *3.238(3)*[e]	*n.a.*	*2.674(2)*	*n.a.*	*2.816(2)*	*2.819(3)*	*2.798(1)*	*2.7366(6)*	*2.9999(5)*
P–Bi$_{calc}$ B3LYP gas [WBI]	3.270 [0.13]	3.308 [0.14][d] 3.295 [0.14][e]	3.084 [0.26]	2.835 [0.49]	2.690 [0.73]	3.020 [0.31]	2.989 [0.33]	3.006 [0.31]	2.851 [0.50]	3.100 [0.25]
P–Bi$_{calc}$ B3LYP CPCM [f] [WBI]	3.269 [0.14]	3.315 [0.14][d] 3.304 [0.14][e]	2.990 [0.34]	2.756 [0.61]	2.693 [0.72]	2.887 [0.44]	2.859 [0.46]	2.874 [0.45]	2.798 [0.59]	3.009 [0.32]
P–Bi$_{calc}$ B3LYP-D3 CPCM [f] [WBI]	3.184 [0.15]	3.201 [0.16][d] 3.180 [0.17][e]	2.997 [0.29]	2.752 [0.55]	2.661 [0.73]	2.857 [0.43]	2.812 [0.48]	2.818 [0.47]	2.758 [0.59]	2.934 [0.35]
Bi–X$_{X\text{-}ray}$	*2.283(7)*[g]	*2.295(8)*[d] *2.348(8)*[e]	*n.a.*	*2.736(4)*[h]	*n.a.*	*2.768(2)*	*2.953(2)*	*3.1980(6)*	*3.0295(3)* *3.1175(3)*[i]	*2.6595(6)*
Bi–X$_{calc}$ B3LYP gas [WBI]	2.315 [0.70]	2.381 [0.68][d] 2.358 [0.67][e]	2.128 [0.36]	2.433 [0.14]	n.a.	2.637 [0.52]	2.831 [0.55]	3.029 [0.62]	3.008 [0.66] 3.320 [0.32][i]	2.672 [0.63]
Bi–X$_{calc}$ B3LYP CPCM [WBI]	2.321 [0.69]	2.321 [0.67][d] 2.360 [0.67][e]	2.192 [0.29]	2.650 [0.08]	n.a.	2.799 [0.35]	3.009 [0.37]	3.210 [0.42]	3.070 [0.58] 3.261 [0.37][i]	2.742 [0.53]
Bi–X$_{calc}$ B3LYP-D3 CPCM [WBI]	2.309 [0.68]	2.308 [0.66][d] 2.318 [0.65][e]	2.113 [0.43]	2.483 [0.13]	n.a.	2.746 [0.39]	2.992 [0.37]	3.188 [0.41]	3.042 [0.58] 3.208 [0.38][i]	2.720 [0.53]
Angles										
P–Bi–X$_{X\text{-}ray}$	*161.5(5)*[g]	*163.6(6)*[d] *165.5(6)*[e]	*n.a.*	*163.1(5)*[h]	*n.a.*	*166.1(6)*	*167.9(8)*	*170.6(3)*	*174.6(3)*[j]	*171.01(2)*
P–Bi–X$_{calc}$ B3LYP gas	165.7	163.8[d] 166.3[e]	161.6	164.1	n.a.	168.2	169.0	171.6	171.4[j]	169.6
P–Bi–X$_{calc}$ B3LYP CPCM	166.0	163.9[d] 166.5[e]	163.1	165.4	n.a.	169.1	169.8	171.9	173.6[j]	170.2

P–Bi–X_{calc} B3LYP-D3 CPCM	160.5	161.2[d] 163.7[e]	160.5	160.8	n.a.	167.0	168.0	170.1	171.0[j]	166.9
peri-region torsion angle Bi1–C1···C9–P9$_{X\text{-}ray}$	*8(1)*	*1(1)[d] 9(1)[e]*	*n.a.*	*3.3(8)*	*n.a.*	*8(1)*	*2(1)*	*4.0(5)*	*1.6(3)*	*5.2(3)*
Splay angle[k]$_{X\text{-}Ray}$	*17.1(9)*	*15(1) and 15(1)*	*n.a.*	*1.4(9)*	*n.a.*	*5(1)*	*5(2)*	*5.3(6)*	*3.6(3)*	*10.0(2)*
Natural Charges q (P / Bi / X) B3LYP CPCM	0.86 / 1.24 / –0.43	0.86 / 1.25 / –0.43	0.89 / 1.48 / –0.80	0.99 / 1.34 / –0.61	1.05 / 1.22 / n.a.	0.94 / 1.28 / –0.74	0.96 / 1.23 / –0.71	0.96 / 1.18 / –0.67	1.00 / 1.06 / –0.52	0.92 / 1.21 / –0.38
Dipole Moments μ gas / B3LYP CPCM	3.1 / 4.0	2.5 / 3.6	7.4 / 10.5	15.4 / 22.1	3.5 / 4.2	9.3 / 14.9	10.2 / 16.2	9.9 / 16.4	0.0 / 0.0	7.3 / 11.2

[a] X-ray values are for **2**·MeCN; [b] Cation of **5** (without BF_4^- counterion); [c] X-ray values are for **9**·$CHCl_3$ (in its dimeric assembly), calculated values are also for the dimeric assembly; [d] values for quasi-linear P···Bi–$C_{(Ph)}$ moiety; [e] values for quasi-linear P···Bi–$C_{(Acenap)}$ moiety; [f] CPCM solvent model (parameters of $CHCl_3$); [g] X = C13; [h] X = F1, the closest atom in BF_4^- anion, *i.e.* involves the non-bonding contact (Bi1···F1); [i] The secondary bonding distance (Bi1···I2') is 3.4723(5) Å (calculated: 3.304 Å for gas, 3.466 Å for CPCM and 3.382 Å for CPCM with dispersion correction), with WBIs of 0.30, 0.24 and 0.25, respectively; [j] P9–Bi1···I2' angle (involves secondary Bi1···I2' interaction in this case); an additional quasi-linear motif (I1–Bi1–I2) is present in this structure, which adopts an angle of 172.171(5)°; [k] Splay angle: the sum of the bay region angles − 360° (see Figure S1 in the Supporting Information).

Because bonding to the heavy pnictogen may also be affected by intramolecular dispersion interactions (which are missing in the standard B3LYP functional), we reoptimized the structures in the continuum with addition of an empirical dispersion correction (Grimme D3 correction, see Supporting Information for details). This led to contraction of the relevant distances by 0.01 – 0.17 Å (compare B3LYP CPCM and B3LYP-D3 CPCM entries in Table 1). In most cases the correction slightly improved the agreement between calculated and experimental structural parameters.

Compound **6** represents the fourth member in the series of Group 15 chloride congeners shown in Figure 2, three of which have been published previously.[23, 30, 41] In this series, there is a distinct difference between both the phosphorus/arsenic and antimony/bismuth congeners and the structural data correlate well with solution δ_P values of the *i*Pr_2P donor group (also shown in Figure 2). In the crystal, the phosphorus congener exists as a phosphino–phosphonium salt with ionically separated Cl^- counterion, with δ_P of 60.0 ppm indicating a rather deshielded phosphorus environment.[41] The observed chemical shift of the arsenic congener (δ_P 58.8 ppm) implies it also exists in the same (ionically separated) form in the $CDCl_3$ solution. However, within the crystal there is a distinct, albeit rather weak, interaction between the arsenic and the chlorine atom (As–Cl 2.9016(8) Å).[30] For the antimony derivative, a significant shift to lower frequency is observed (δ_P 1.5 ppm). This is consistent with the notion that the ionic character is significantly decreased (Sb–Cl distance is 2.6798(8) Å), *i.e.* less electron density is being transferred from the phosphorus (donor) to the antimony atom.[23] These observations are corroborated by calculations, which reveal the covalent P−E WBIs decrease along the series of chloride congeners shown in Figure 2 (E = P: 0.90, As: 0.71, Sb: 0.50, Bi: 0.44). Following these observations and calculations it would be expected that the bismuth congener would show a low frequency shift in the $^{31}P\{^1H\}$ NMR spectrum. However, this is not the case as there is a slight shift to higher frequency on changing from the antimony (δ_P 1.5 ppm) to the bismuth congener (δ_P 18.8 ppm). This is unlikely to be attributed to a more pronounced transfer of the phosphorus lone pair density towards bismuth. Instead, we believe the prevalence of relativistic effects,[42] due to spin-orbit contributions, analogous to Inverse Halogen Dependence (IHD), result in this unexpected ^{31}P chemical shift value observed for the heaviest (Bi) congener.

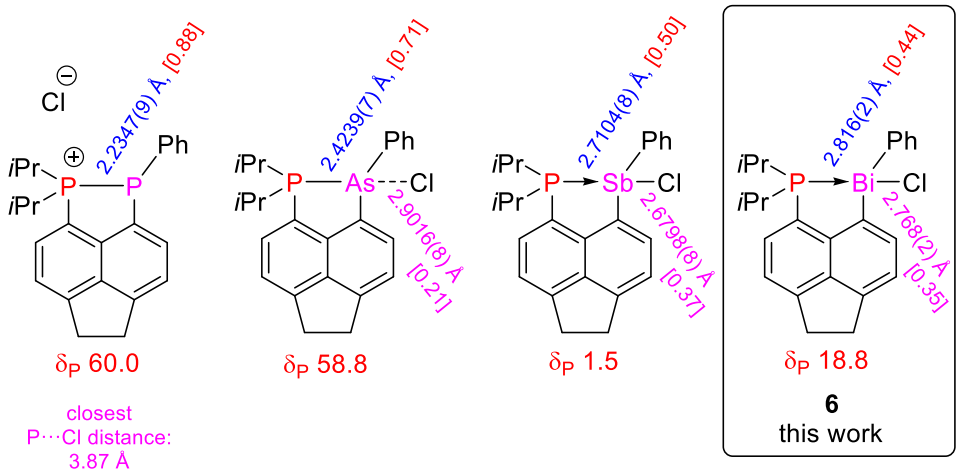

Figure 2: The Group 15 congeners of chloride **6**. Relevant structural parameters (X-ray diffraction) and δ_P (in ppm) for iPr$_2$P group are shown.[23, 30, 41] Calculated WBI values of P–E and E–Cl bonds (E = P, As, Sb, Bi) are shown in square brackets, for details see Table S3 in SI.

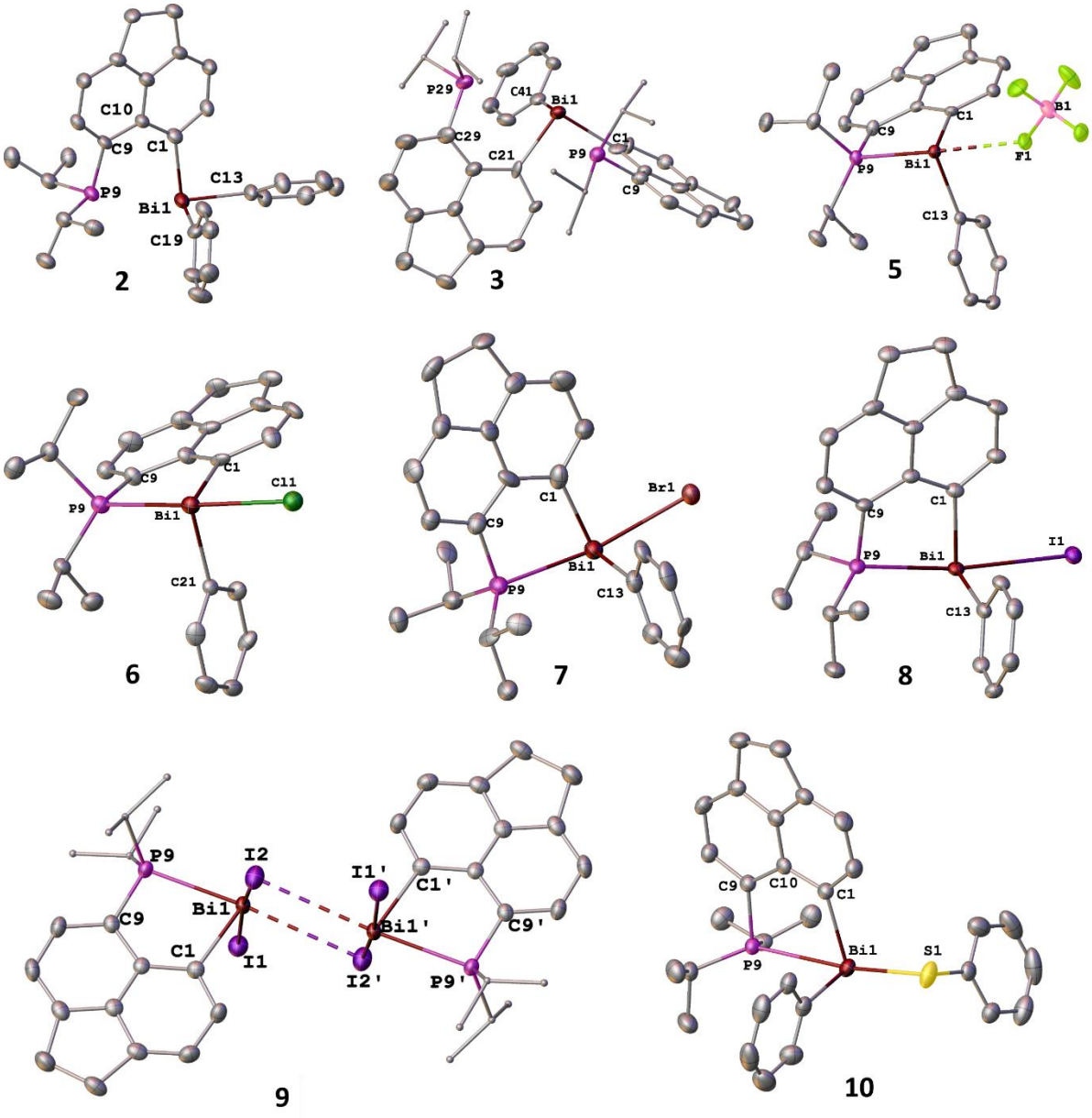

Figure 3: Crystal structures of **2**, **3** and **5**–**10**. Hydrogen atoms and solvating molecules (MeCN in **2**, $CHCl_3$ in **9**) are omitted. Thermal ellipsoids are plotted at the 50% level, isopropyl groups in **3** and **9** are drawn in wireframe for clarity.

Geminally Bis(acenaphthyl) Substituted Species 3

Both Ph_2BiCl and $PhBiCl_2$ have been prepared by redistribution reactions of $BiPh_3$ and $BiCl_3$ using the appropriate ratios.[32-33] However, the preparation of $PhBiCl_2$ proved to be significantly more difficult than that of Ph_2BiCl. Despite multiple attempts, the $PhBiCl_2$ produced was contaminated by

Ph_2BiCl (*ca*. 15% as detected by ^1H NMR). The purity of the material did not improve on recrystallisation.

Following the same general procedure as for the preparation of **2**, the impure $PhBiCl_2$ was reacted with two equivalents of **1** (Scheme 1). Aqueous workup and recrystallisation from MeCN yielded a mixture of the desired product **3** and several unknown byproducts. Recrystallisation did not improve purity of **3** significantly, as judged by ^1H and ^{31}P NMR spectroscopy. Hence, an alternative synthetic pathway was developed, using **6** as an intermediate. The reaction of **6** with **1** proceeded cleanly, giving pure **3** in a 62% yield after recrystallisation from MeCN (Scheme 1).

The lighter congeners of **3**, with a general formula of $(Acenap(PiPr_2))_2EPh$ (E = As, Sb), have been reported by us previously.[24] They display restricted molecular movements on the NMR timescale, which are observable through broadening of both their ^1H and $^{31}P\{^1H\}$ NMR signals. In the $^{31}P\{^1H\}$ NMR spectra of the As and Sb congeners, anisochronous signals for the phosphorus atoms were observed below or at room temperature, and isochronous patterns are observed at elevated temperatures. Energy barriers, $\Delta G^{\ddagger}$, for the relevant interchange process (rotation around $E–C_{acenap}$ bond), determined by the coalescence method, were found to be 62.3 kJ mol^{-1} for the arsenic derivative at 340 K, and 62.0 kJ mol^{-1} for the antimony congener at 303 K.

The room temperature $^{31}P\{^1H\}$ NMR spectrum of **3** at 202 MHz shows a singlet at δ_P –22.9 ppm, which is only slightly broadened (Figure 4, top). This indicates **3** is in the fast exchange regime at room temperature, with the two phosphorus atoms being isochronous. The low temperature (slow motion regime) $^{31}P\{^1H\}$ NMR spectrum of **3** at 185 K displays two sharp doublets at δ_P −24.9 and −28.9 ppm, with $^{8ts}J_{PP}$ 17.8 Hz (Figure 4, bottom), consistent with a simple AX spin system. The magnitude of the $^{8ts}J_{PP}$ is remarkable as a direct overlap of the lone pairs on the phosphorus atoms is unlikely due to the steric clashes this would generate. Therefore, the transfer of magnetisation in **3** likely involves two P···Bi through-space interactions via the lone pair on the bismuth atom as shown in Figure 5.

The $^{31}P\{^1H\}$ signals of **3** coalesce at 262 K (at 202 MHz, see Figure 4), which corresponds to a rotational barrier of $\Delta G^{\ddagger}$ = 47.6 kJ mol^{-1}. Whilst the values for each pnictogen containing compound are not directly comparable due to the use of the coalescence method, the larger size and polarizability of the bismuth atom is expected to result in a slightly lower barrier compared to the antimony and arsenic derivatives.

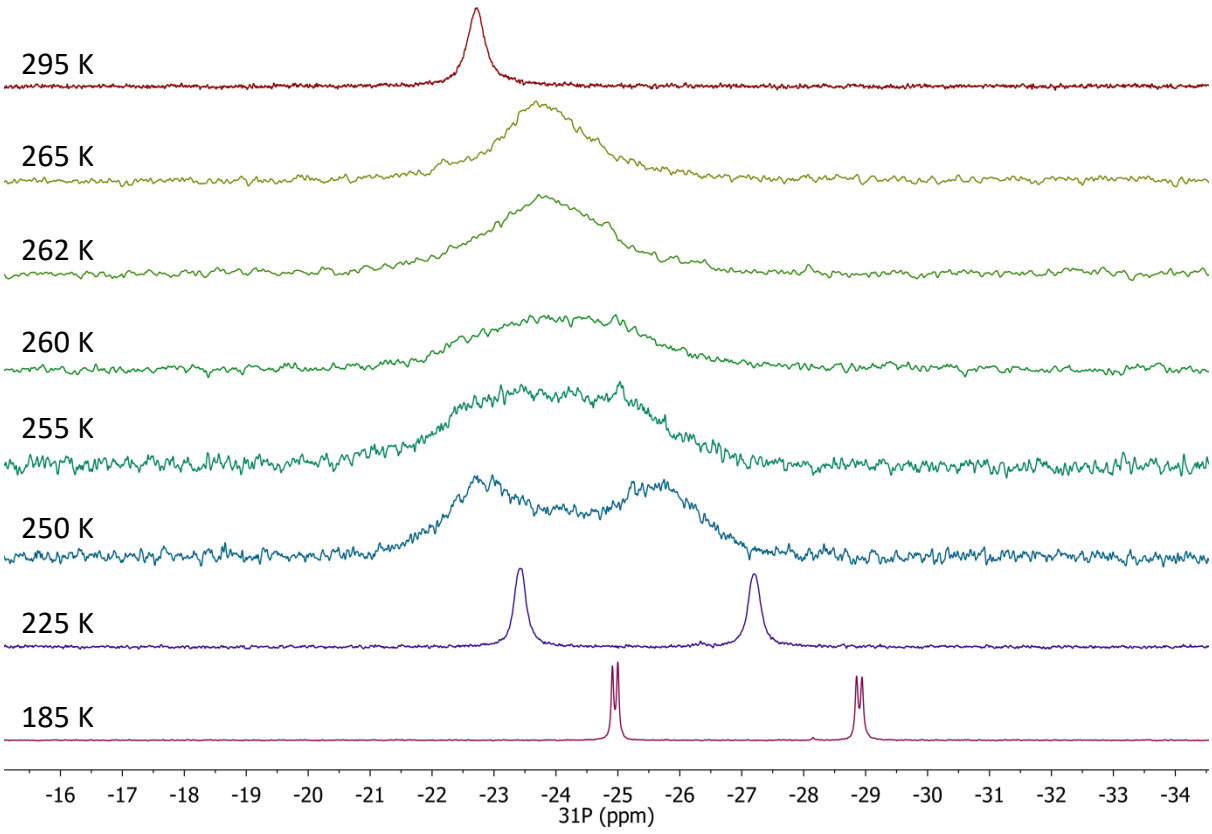

Figure 4: Variable temperature $^{31}P\{^{1}H\}$ NMR spectra of **3** (CD_2Cl_2, 202 MHz).

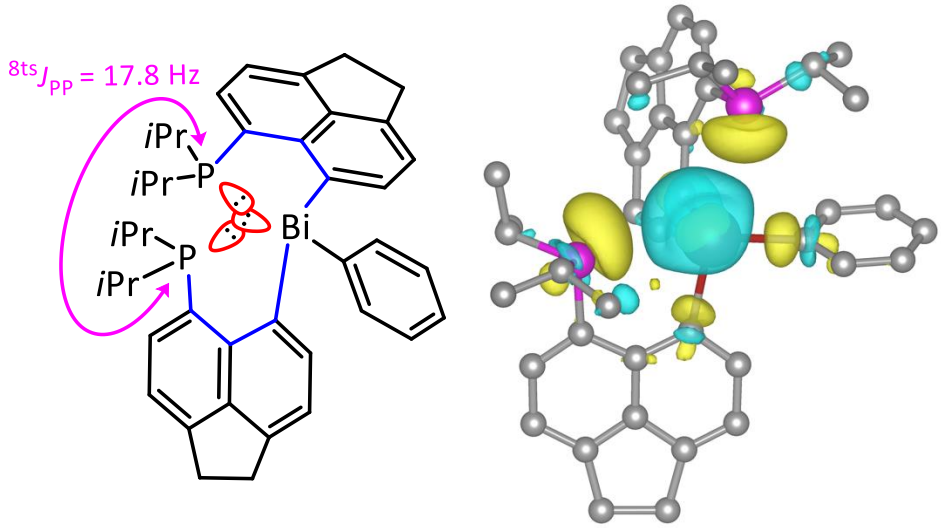

Figure 5: Left: Graphical representation of the magnetisation transfer pathway in **3** for long-range $^{8ts}J_{PP}$ coupling. The shortest bond pathway is coloured blue, with the three lone pairs involved in the (through-space) transfer of magnetisation coloured red. Right: CDD isosurface plot of J_{PP} in **3'**$_{solid}$ at a contour level of 1.05. Areas in cyan exhibit reduced charge density and areas in yellow an increased charge density as a result of the Fermi-contact *J* coupling in the non-relativistic regime. Hydrogen atoms omitted for clarity.

A clear trend can be observed in the δ_P chemical shifts of the arsenic, antimony and bismuth analogues of **3** in the fast motion regime; the P atom in the bismuth congener **3** is the most shielded in the series (δ_P −10.5 (As, 373 K, d_8-toluene), −17.5 (Sb, 363 K, d_8-toluene), −22.9 ppm (Bi (**3**), 298 K, $CDCl_3$)). The $^{13}C\{^1H\}$ NMR spectrum of **3** shows a triplet for the *ipso*-carbon of the phenyl ring with a large coupling constant of $^{5ts}J_{CP}$ = 34.7 Hz, stemming from (through-space) coupling with the two phosphorus atoms.

The crystal structure of **3** is shown in Figure 3 with selected structural parameters listed in Table 1. Within the structure of **3**, neither of the phosphorus atoms forms a conventional dative bond with the bismuth centre. The P···Bi distances are 3.227(2) and 3.238(2) Å, which is only slightly shorter than in the less crowded molecule **2** (3.263(2)) Å. Considering the quasi-linear arrangement of the P···Bi–C bonds in **3** (P9···Bi1–C41 163.6(6)°, P29···Bi1–C1 165.5(6)°) and the sub-van der Waals P···Bi distances, weak 3c–4e n(P)→σ*(Bi–C) interactions may contribute to the conformation observed in the crystal structure. There are moderate out-of-plane distortions in the *peri*-regions of molecule **3**, with the acenaphthene backbone P–C···C–Bi torsion angles of 1(1)° and 9(1)°, and out-of-plane displacements from the mean acenaphthene plane of around 0.17–0.22 Å for both the phosphorus and bismuth atoms. However, the in-plane distortions are more significant as indicated by the large P···Bi separations (discussed above) and positive splay angles (both 15(1)°).

A periodic planewave density functional theory (DFT) study was performed on the solid-state structure of **3** in order to gain additional understanding of the mechanisms of the observed *J* couplings. **3** was computed as an isolated molecule, extracted from the experimentally obtained crystal structure and placed in a 10 × 10 × 10 Å box, denoted **3'$_{isol}$**, and as the full crystal structure (Z = 2, Z' = 1, P-1), **3'$_{solid}$**. **3'$_{isol}$** and **3'$_{solid}$** were subjected to geometry optimization under DFT forces, the former with a fixed unit cell and the latter with the unit cell relaxed under DFT stresses. The geometries computed for **3'$_{isol}$** and **3'$_{solid}$** (Table S4 in the SI) were in good agreement with experimental single crystal X-ray diffraction data, as well as computed structures in the gas phase and under implicit solvation (see Table 1).

Table 2. Selected *J* couplings [Hz] computed for **3'$_{isol}$** and **3'$_{solid}$**.

	3'$_{isol}$	**3'$_{solid}$**
J_{PP}	34.7	17.7
$J_{PC(Ph)}$	75.2	70.7
J_{PBi}	1520	1360

The total *J* coupling values computed for **3'$_{isol}$** and **3'$_{solid}$** are given in Table 2; a breakdown of the contributing components of the isotropic *J* coupling is given in Table S5 in the SI. Calculations for **3'$_{solid}$** adopted a 2 × 2 × 1 supercell to mitigate interactions between the perturbing nucleus and periodic images. Because it is free from packing forces, **3'**$_{isol}$ is probably a better model for the structure in solution than **3'$_{solid}$**, however the computed NMR parameters are qualitatively similar for both systems. The computed values J_{PP} = 34.7 and 17.7 Hz are in fair to excellent agreement with J_{PP} = 17.8 Hz found experimentally for the low-temperature AX spin system by variable temperature $^{31}P\{^{1}H\}$ NMR. However, the computed $J_{PC(Ph)}$ = 75.2 and 70.7 Hz overestimate the room-temperature solution-state NMR value (34.7 Hz) by over 100%. This suggests that the intramolecular motion reduces the magnitude of such interactions as previously observed in a solid-state NMR study of related molecular crystals.[43]

To confirm the *J* coupling between the ^{31}P nuclei in **3** is through-space, **3'$_{solid}$** was subjected to coupling deformation density (CDD) calculations, which map the change in charge density due to the Fermi-contact *J* coupling interaction in the non-relativistic regime.[44-45] It should be noted that while the *J* couplings in **3** are Fermi-contact dominated, they are likely subject to relativistic effects due to the mass of Bi, and so the CDD plot in this case provides a qualitative understanding only. A CDD plot for J_{PP} in **3'$_{solid}$** is given in Figure 5 (right) as an isosurface. It shows charge density around the ^{209}Bi is reduced and around the ^{31}P nuclei is increased. This is in good agreement with the notion that the P and Bi lone pairs mediate communication between the two ^{31}P nuclei. This notion is also supported by a recent solid state NMR study of through space P···Bi couplings, involving coupling transfer through lone pairs on P and Bi atoms in accordion-like compounds.[46] These have shown large magnitudes of J_{PBi} despite having even longer P–Bi distances (ranging from 3.365(1) to 3.792(9) Å) than those observed in the crystal structure of **3** (3.227(2) and 3.238(3) Å).

Reactions of Acenap(P*i*Pr$_2$)Li (**1**) with $BiCl_3$ and BiI_3

For completeness, the reactivity of **1** with $BiCl_3$ was also investigated. The reaction of **1** with ⅓ equivalent of $BiCl_3$ yielded geminally tris(acenaphthyl) substituted (Acenap(P*i*Pr$_2$))$_3$Bi **11** in good purity, albeit in a relatively low yield (Scheme 2). The compound was fully characterised (including single crystal X-ray diffraction) and reported together with other propeller-shaped molecules in a recent paper.[27]

The phosphine–dichlorobismuthine complex **12** (Scheme 2) is of significant interest as a prospective synthon as it possesses two synthetically versatile Bi–Cl functionalities. Our attempts to synthesise **12** by slow addition of **1** to one equivalent of $BiCl_3$ at –78 °C yielded a suspension. The solid was difficult to analyse by solution state NMR due to its insolubility in common organic solvents. Attempts to purify the product by recrystallization were unsuccessful, mostly leading to decomposition to a black solid, suggesting that **11** is rather thermally unstable. This is a disappointing result, considering that the synthesis of the closely related Acenap(PPh_2)($BiCl_2$) has been reported by Beckmann, including the single crystal X-ray data.[15]

Nonetheless, an alternative target compound of similar synthetic utility has been identified, phosphine–diiodobismuthine complex **9**. During one of the attempts to obtain crystals of compound **8** from the mixture after the reaction of **5** with aqueous NaI, a crystal of a different morphology was obtained alongside those of **8**. This yellow crystal was subjected to single crystal X-ray diffraction, which revealed it to be the dative species **9** in the form of its $CHCl_3$ solvate (Scheme 1).

The apparent stability of the diiodobismuthine **9** prompted us to explore rational synthetic routes to it. Two different pathways were investigated as shown in Scheme 2 (further details given in the SI). Unfortunately, neither of the synthetic routes produced **9** in good purity; nevertheless, **9** appears to be one of the major products formed in both syntheses.

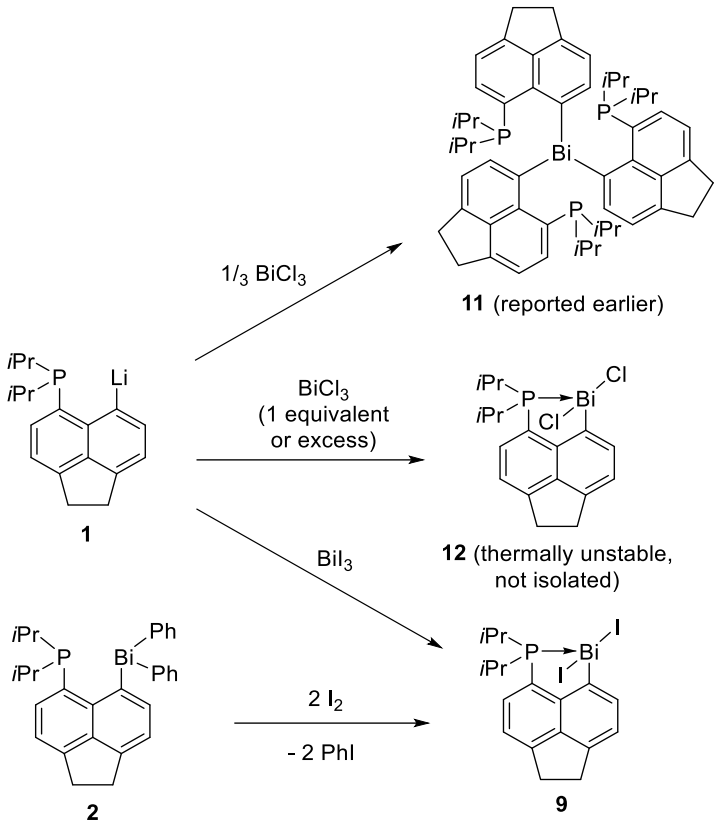

Scheme 2: Reactions of **1** with $BiCl_3$ at various stoichiometries and attempted routes to **9**.

Crystals of **9** were obtained in the form of three different solvates (**9**·$CHCl_3$, **9**·CH_2Cl_2 and **9**·THF) and were subjected to single crystal X-ray diffraction. The molecular geometry of **9** is essentially the same in all three crystal structures; hence only data of **9**·$CHCl_3$ are discussed below (as those are the highest quality). Details of all three solvate structures are given in Table S1 in the SI.

The structure of **9**·$CHCl_3$ is shown in Figure 3 with selected structural parameters in Table 1. The compound forms a centrosymmetric dimer via bridging iodine atoms. Similar dimers have been observed for other related pnictogen dihalides, such as Acenap(PPh_2)($BiCl_2$), Acenap(P*i*Pr_2)($AsCl_2$) and Acenap(P*i*Pr_2)($SbCl_2$).[15, 23, 47]

Formally, **9** represents a phosphine-donor bismuthine-acceptor complex of a general formula $R_3P\rightarrow BiR_3$. The relatively high Lewis acidity of halobismuthines BiX_3 and $BiRX_2$ means that complexes with phosphine donors are stable, even without the additional supporting backbone holding the P and Bi centres in close proximity. Examples include the dimeric complexes [$BiCl_3$(dppm)]$_2$ (dppm = bis(diphenylphosphino)methane)[17] and [$BiBr_3$·(dppe)]$_2$ (dppe = 1,2-

bis(diphenylphosphino)ethane),[18] tetrameric $[BiBr_3 \cdot PEt_3]_4$,[18] amongst others.[11] However, we did not find in the literature any examples of structurally characterised organodiiodo bismuthine complexes with phosphine donors (general formula $R_3P \rightarrow RBiI_2$). Only complexes with amine donors ($R_3N \rightarrow RBiI_2$) were reported; in all cases the amine groups were linked to the bismuth centre via an organic backbone.[48-50] This may reflect the lower stability of the $R_3P \rightarrow RBiI_2$ complexes resulting from lower Lewis acidity of organodiiodobismuthines compared to, for example, bismuth trihalides.

The phosphorus atom in **9** adopts a tetrahedral geometry, donating its lone pair to the bismuth atom, which consequently adopts a pseudo-octahedral geometry, with its lone pair occupying one of the octahedral sites. A secondary Bi···I interaction (3.472(1) Å) links the two molecules in the dimer. The P–Bi bond length in **9** (2.7366(6) Å) is close to the "conventional" P–Bi covalent bond length, such as that seen in **5** (2.674(2) Å). The I1–Bi1–I2 motif is close to linear (172.171(5)°). The Bi1–I2 bond (3.1175(3) Å) is slightly longer than the Bi1–I1 bond (3.0295(3) Å), owing to atom I2 acting as a bridge in the formation of the dimer. Overall, the geometry of the acenaphthene backbone in **9** is rather relaxed, with minimum in- and out-of-plane distortions of the acenaphthene plane (see Table 1).

Conclusions

A selective dearylation of phosphine−bismuthine **2** has been developed in this work. It allowed access to a series of novel species containing relatively rare P–Bi bonds. While air and moisture sensitive, many of the reported compounds are rather thermally stable (for example, diffraction quality crystals of **9** were obtained from boiling THF). This appears remarkable considering the position of Bi at the heel of Group 15 and the commonly adopted notion that bonding weakens progressively on descent of the groups.

Synthesis and full characterisation of the last missing congener (**6**) in the series of phosphine−chloropnictine acenaphthene species Acenap(P*i*Pr$_2$)(PnPhCl) allowed correlation of their structural parameters and ^{31}P NMR chemical shifts. For lighter elements (P, As and Sb congeners), the δ_P is proportional to the amount of electron density being transferred to the acceptor (strength of the dative P→E interaction). The trend is disturbed in the case of the bismuth species **6**, with spin-orbit contributions (relativistic effects) being the likely reason.

Investigations into fluxional processes of bis(acenaphthene) species **3** were corroborated with DFT calculations. These demonstrated a through-space magnetisation transfer pathway leading

to a long-range double through-space $^{8ts}J_{PP}$ coupling of 17.8 Hz, with the lone pair on the bismuth atom serving as a magnetisation relay.

Associated Content

Supporting Information

The Supporting Information is available free of charge at https://pubs.acs.org/doi/XXX.

Experimental, including general considerations, synthetic methods, exploration of rational synthetic routes to diiodobismuthine **9**, X-ray diffraction and computational details.

Research Data

The research data underpinning this publication can be accessed at https://doi.org/10.17630/39edc339-fbac-402e-9034-cfaa44a34251.

Accession Codes

CCDC 1948146-1948155 contain the supplementary crystallographic data for this paper. These data can be obtained free of charge via www.ccdc.cam.ac.uk/data_request/cif, or by emailing data_request@ccdc.cam.ac.uk, or by contacting The Cambridge Crystallographic Data Centre, 12 Union Road, Cambridge CB2 1EZ, UK; fax: +44 1223 336033.

Author Information

Corresponding Author

Petr Kilian E-mail: pk7@st-andrews.ac.uk orcid.org/0000-0001-6379-3026

Other Authors

Phillip S. Nejman

Thomasine E. Curzon

Michael Bühl orcid.org/0000-0002-1095-7143

David McKay orcid.org/0000-0003-0362-7848

J. Derek Woollins orcid.org/0000-0002-1498-9652

Sharon E. Ashbrook orcid.org/0000-0002-4538-6782

David B. Cordes orcid.org/0000-0002-5366-9168

Alexandra M. Z. Slawin orcid.org/0000-0002-9527-6418

Author Contributions

The manuscript was written through contributions of all authors. All authors have given approval to the final version of the manuscript.

Notes

The authors declare no competing financial interest

Acknowledgements

This work was financially supported by the Engineering and Physical Sciences Research Council (EPSRC). This included PhD studentship to TEC (Centre for Doctoral Training in Critical Resource Catalysis (CRITICAT), Grant code: EP/L016419/1) and to PN (Grant code EP/L505079/1). The authors would like to thank COST action SM1302 SIPs; the EPSRC UK National Mass Spectrometry Facility at Swansea University for the acquisition and processing of Mass Spectrometry Data and to EaStCHEM and the School of Chemistry for support. MB would like to thank Dr H. Früchtl for technical assistance with the computations. DM would like to thank Professor J. R. Yates for provision of the CASTEP CDD code. PK and TEC would like to thank Dr D. Dawson for acquisition of solid state NMR spectra.

References

1. Kannan, R.; Kumar, S.; Andrews, A. P.; Jemmis, E. D.; Venugopal, A., Consequence of Ligand Bite Angle on Bismuth Lewis Acidity. *Inorganic Chemistry* **2017,** *56* (16), 9391-9395.
2. Ramler, J.; Hofmann, K.; Lichtenberg, C., Neutral and Cationic Bismuth Compounds: Structure, Heteroaromaticity, and Lewis Acidity of Bismepines. *Inorganic Chemistry* **2019**.
3. Sanderson, J.; Bayse, C. A., The Lewis acidity of bismuth(III) halides: a DFT analysis. *Tetrahedron* **2008,** *64* (33), 7685-7689.

4. Benjamin, S. L.; Reid, G., Neutral organoantimony(III) and organobismuth(III) ligands as acceptors in transition metal complexes – Role of substituents and co-ligands. *Coordination Chemistry Reviews* **2015,** *297-298*, 168-180.
5. Benjamin, S. L.; Levason, W.; Reid, G.; Warr, R. P., Halostibines SbMeX2 and SbMe2X: Lewis Acids or Lewis Bases? *Organometallics* **2012,** *31* (3), 1025-1034.
6. Benjamin, S. L.; Karagiannidis, L.; Levason, W.; Reid, G.; Rogers, M. C., Hybrid Dibismuthines and Distibines: Preparation and Properties of Antimony and Bismuth Oxygen, Sulfur, and Nitrogen Donor Ligands. *Organometallics* **2011,** *30* (4), 895-904.
7. Gerhard Muller, H.-J. M., Martin Winkler, Donor-Acceptor Complexes between Simple Phosphines. First Structural Data for an Almost Forgotten Class of Compounds. *Zeitschrift fur Naturforschung B: Journal of Chemical Sciences* **2001,** *56b* (11), 1155-1162.
8. Chitnis, S. S.; Vos, K. A.; Burford, N.; McDonald, R.; Ferguson, M. J., Distinction between coordination and phosphine ligand oxidation: interactions of di- and triphosphines with Pn3+ (Pn = P, As, Sb, Bi). *Chemical Communications* **2016,** *52* (4), 685-688.
9. Levason, W.; McAuliffe, C. A., Phosphorus, arsenic and antimony complexes of the main group elements. *Coordination Chemistry Reviews* **1976,** *19* (2), 173-185.
10. Norman, N. C.; Pickett, N. L., Phosphine complexes of the heavier p-block elements: aspects of structure and bonding. *Coordination Chemistry Reviews* **1995,** *145* (0), 27-54.
11. Burt, J.; Levason, W.; Reid, G., Coordination chemistry of the main group elements with phosphine, arsine and stibine ligands. *Coordination Chemistry Reviews* **2014,** *260* (0), 65-115.
12. Robertson, A. P. M.; Gray, P. A.; Burford, N., Interpnictogen Cations: Exploring New Vistas in Coordination Chemistry. *Angewandte Chemie-International Edition* **2014,** *53* (24), 6050-6069.
13. Chitnis, S. S.; Burford, N., Phosphine complexes of lone pair bearing Lewis acceptors. *Dalton Transactions* **2015,** *44* (1), 17-29.
14. Raţ, C. I.; Silvestru, C.; Breunig, H. J., Hypervalent organoantimony and -bismuth compounds with pendant arm ligands. *Coordination Chemistry Reviews* **2013,** *257* (5), 818-879.
15. Hupf, E.; Lork, E.; Mebs, S.; Chęcińska, L.; Beckmann, J., Probing Donor–Acceptor Interactions in peri-Substituted Diphenylphosphinoacenaphthyl–Element Dichlorides of Group 13 and 15 Elements. *Organometallics* **2014,** *33* (24), 7247-7259.
16. Chitnis, S. S.; Burford, N.; Decken, A.; Ferguson, M. J., Coordination Complexes of Bismuth Triflates with Tetrahydrofuran and Diphosphine Ligands. *Inorganic Chemistry* **2013,** *52* (12), 7242-7248.
17. Willey, G. R.; Daly, L. T.; Drew, M. G. B., Phosphorus donor complexes of bismuth(III). Structural characterisation of [Bi2Cl6(Ph2PCH2PPh2)2], [Bi2Cl6(Ph2PCH2CH2PPh2)2] and [Bi2Cl6(Ph2PCH2CH2PPh2)3]. *Journal of the Chemical Society, Dalton Transactions* **1996,** (6), 1063-1067.
18. Clegg, W.; Elsegood, M. R. J.; Graham, V.; Norman, N. C.; Pickett, N. L.; Tavakkoli, K., Neutral phosphine complexes of antimony(III) and bismuth(III) halides. *Journal of the Chemical Society, Dalton Transactions* **1994,** (12), 1743-1751.
19. Clegg, W.; John Errington, R.; Fisher, G. A.; Green, M. E.; Hockless, D. C. R.; Norman, N. C., A Phosphine Complex of Bismuth(III): X-ray Crystal Structure of [PMe3H][Bi2Br7(PMe3)2]. *Chemische Berichte* **1991,** *124* (11), 2457-2459.
20. Chitnis, S. S.; Burford, N.; McDonald, R.; Ferguson, M. J., Prototypical Phosphine Complexes of Antimony(III). *Inorganic Chemistry* **2014,** *53* (10), 5359-5372.
21. Kilian, P.; Knight, F. R.; Woollins, J. D., Naphthalene and Related Systems peri-Substituted by Group 15 and 16 Elements. *Chemistry-a European Journal* **2011,** *17* (8), 2302-2328.
22. Kilian, P.; Knight, F. R.; Woollins, J. D., Synthesis of ligands based on naphthalene peri-substituted by Group 15 and 16 elements and their coordination chemistry. *Coordination Chemistry Reviews* **2011,** *255* (11-12), 1387-1413.

23. Chalmers, B. A.; Bühl, M.; Athukorala Arachchige, K. S.; Slawin, A. M. Z.; Kilian, P., Structural, Spectroscopic and Computational Examination of the Dative Interaction in Constrained Phosphine–Stibines and Phosphine–Stiboranes. *Chem. Eur. J.* **2015,** *21* (20), 7520-7531.
24. Chalmers, B. A.; Meigh, C. B. E.; Nejman, P. S.; Buhl, M.; Lebl, T.; Woollins, J. D.; Slawin, A. M. Z.; Kilian, P., Geminally Substituted Tris(acenaphthyl) and Bis(acenaphthyl) Arsines, Stibines, and Bismuthine: A Structural and Nuclear Magnetic Resonance Investigation. *Inorganic Chemistry* **2016,** *55*, 7117-7125.
25. Groom, C. R.; Bruno, I. J.; Lightfoot, M. P.; Ward, S. C., The Cambridge Structural Database. *Acta Crystallographica Section B* **2016,** *72* (2), 171-179.
26. Olaru, M.; Krupke, S.; Lork, E.; Mebs, S.; Beckmann, J., Transmetallation of bis(6-diphenylphosphinoxy-acenapth-5-yl)mercury with tin tetrachloride, antimony trichloride and bismuth trichloride. *Dalton Transactions* **2019,** *48* (17), 5585-5594.
27. Chalmers, B. A.; Meigh, C. B. E.; Nejman, P. S.; Bühl, M.; Lébl, T.; Woollins, J. D.; Slawin, A. M. Z.; Kilian, P., Geminally Substituted Tris(acenaphthyl) and Bis(acenaphthyl) Arsines, Stibines, and Bismuthine: A Structural and Nuclear Magnetic Resonance Investigation. *Inorganic Chemistry* **2016,** *55* (14), 7117-7125.
28. Wade, C. R.; Saber, M. R.; Gabbaï, F. P., Synthesis and structure of peri-substituted boron/pnictogen naphthalene derivatives. *Heteroatom Chemistry* **2011,** *22* (3-4), 500-505.
29. Wielandt, J. W.; Petrie, S.; Kilah, N. L.; Willis, A. C.; Dewhurst, R. D.; Belaj, F.; Orthaber, A.; Stranger, R.; Wild, S. B., Self-Assembly of Square-Planar Halide Complexes of Trimethylphosphine-Stabilized Diphenyl-Arsenium, -Stibenium, and -Bismuthenium Hexafluorophosphates*. *Aust. J. Chem.* **2016,** *69* (5), 524-532.
30. Taylor, L. J.; Buhl, M.; Chalmers, B. A.; Ray, M. J.; Wawrzyniak, P.; Walton, J. C.; Cordes, D. B.; Slawin, A. M. Z.; Woollins, J. D.; Kilian, P., Dealkanative Main Group Couplings across the peri-Gap. *J Am Chem Soc* **2017,** *139* (51), 18545-18551.
31. Quin, L. D., *A Guide to Organophosphorus Chemistry*. Wiley Interscience: New York, 2000.
32. Barton, D. H. R.; Bhatnagar, N. Y.; Finet, J.-P.; Motherwell, W. B., Pentavalent organobismuth reagents. Part vi. Comparative migratory aptitudes of aryl groups in the arylation of phenols and enols by pentavalent bismuth reagents. *Tetrahedron* **1986,** *42* (12), 3111-3122.
33. Karsch, H. H., *Synthetic Methods of Organometallic and Inorganic Chemistry Vol 3: Phosphorus, Arsenic, Antimony and Bismuth*. Thieme: New York, 1996; Vol. 3.
34. C. James, S.; C. Norman, N.; Guy Orpen, A., Pyridine adducts of arylbismuth(III) halides. *Journal of the Chemical Society, Dalton Transactions* **1999,** (16), 2837-2843.
35. Batsanov, S. S., Van der Waals Radii of Elements. *Inorganic Materials* **2001,** *37* (9), 871-885.
36. Suzuki, H.; Murafuji, T.; Matano, Y.; Azuma, N., Chiral chlorobismuthines stabilized by the intramolecular coordination of an N,N-dimethylamino group: X-ray structure analysis, asymmetric induction at the bismuth centre, and dynamic behaviour in solution. *Journal of the Chemical Society, Perkin Transactions 1* **1993,** (23), 2969-2973.
37. Whitmire, K. H.; Labahn, D.; Roesky, H. W.; Noltemeyer, M.; Sheldrick, G. M., Sterically crowded aryl bismuth compounds: synthesis and characterization of bis{2,4,6-tris(trifluoromethyl)phenyl} bismuth chloride and tris{2,4,6-tris(trifluoromethyl)phenyl} bismuth. *Journal of Organometallic Chemistry* **1991,** *402* (1), 55-66.
38. Ebert, K. H.; Schulz, R. E.; Breunig, H. J.; Silvestru, C.; Haiduc, I., Syntheses and structures of dimesitylbismuth(III) bromide, Mes2BiBr, and bis(diphenyldithiophosphinato)mesitylbismuth(III), MesBi(S2PPh2)2. *Journal of Organometallic Chemistry* **1994,** *470* (1), 93-98.
39. Athukorala Arachchige, K. S.; Sanz Camacho, P.; Ray, M. J.; Chalmers, B. A.; Knight, F. R.; Ashbrook, S. E.; Bühl, M.; Kilian, P.; Slawin, A. M. Z.; Woollins, J. D., Sterically Restricted Tin Phosphines, Stabilized by Weak Intramolecular Donor–Acceptor Interactions. *Organometallics* **2014,** *33* (10), 2424-2433.

40. Wiberg, K. B., Application of the pople-santry-segal CNDO method to the cyclopropylcarbinyl and cyclobutyl cation and to bicyclobutane. *Tetrahedron* **1968,** *24* (3), 1083-1096.
41. Ray, M. J.; Slawin, A. M. Z.; Bühl, M.; Kilian, P., peri-Substituted Phosphino-Phosphonium Salts: Synthesis and Reactivity. *Organometallics* **2013,** *32* (12), 3481-3492.
42. Kaupp, M.; Malkina, O. L.; Malkin, V. G.; Pyykkö, P., How Do Spin – Orbit - Induced Heavy - Atom Effects on NMR Chemical Shifts Function? Validation of a Simple Analogy to Spin – Spin Coupling by Density Functional Theory (DFT) Calculations on Some Iodo Compounds. *Chemistry – A European Journal* **1998,** *4* (1), 118-126.
43. Sanz Camacho, P.; McKay, D.; Dawson, D. M.; Kirst, C.; Yates, J. R.; Green, T. F. G.; Cordes, D. B.; Slawin, A. M. Z.; Woollins, J. D.; Ashbrook, S. E., Investigating Unusual Homonuclear Intermolecular "Through-Space" J Couplings in Organochalcogen Systems. *Inorganic Chemistry* **2016,** *55* (21), 10881-10887.
44. Malkina, O. L.; Malkin, V. G., Visualization of Nuclear Spin–Spin Coupling Pathways by Real-Space Functions. *Angewandte Chemie International Edition* **2003,** *42* (36), 4335-4338.
45. Sanz Camacho, P.; Athukorala Arachchige, K. S.; Slawin, A. M. Z.; Green, T. F. G.; Yates, J. R.; Dawson, D. M.; Woollins, J. D.; Ashbrook, S. E., Unusual Intermolecular "Through-Space" J Couplings in P–Se Heterocycles. *J. Am. Chem. Soc.* **2015,** *137* (19), 6172-6175.
46. Mokrai, R.; Barrett, J.; Apperley, D. C.; Batsanov, A. S.; Benko, Z.; Heift, D., Weak Pnictogen Bond with Bismuth: Experimental Evidence Based on Bi-P Through-Space Coupling. *Chemistry* **2019,** *25* (16), 4017-4024.
47. Chalmers, B. A.; Bühl, M.; Athukorala Arachchige, K. S.; Slawin, A. M. Z.; Kilian, P., Geometrically Enforced Donor-Facilitated Dehydrocoupling Leading to an Isolable Arsanylidine-Phosphorane. *Journal of the American Chemical Society* **2014,** *136* (17), 6247-6250.
48. Soran, A.; Breunig, H. J.; Lippolis, V.; Arca, M.; Silvestru, C., Monoorganobismuth(iii) dihalides containing the new pincer 2,6-{MeN(CH2CH2)2NCH2}2C6H3 ligand: solution NMR, vibrational and single-crystal X-ray studies. *Dalton Transactions* **2009,** (1), 77-84.
49. Carmalt, C. J.; Cowley, A. H.; Culp, R. D.; Jones, R. A.; Kamepalli, S.; Norman, N. C., Synthesis and Structures of Intramolecularly Base-Coordinated Group 15 Aryl Halides. *Inorganic Chemistry* **1997,** *36* (13), 2770-2776.
50. Soran, A. P.; Silvestru, C.; Breunig, H. J.; Balázs, G.; Green, J. C., Organobismuth(III) Dihalides with T-Shaped Geometry Stabilized by Intramolecular N→Bi Interactions and Related Diorganobismuth(III) Halides. *Organometallics* **2007,** *26* (5), 1196-1203.

For Table of Contents Only

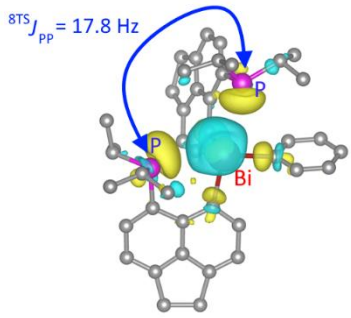

A through-space magnetisation transfer pathway leading to a long-range double through-space $^{8ts}J_{PP}$ coupling of 17.8 Hz was identified. The coupling pathway includes the lone pair on the bismuth atom, which serves as a magnetisation relay.